UNIVERSITY OF COPENHAGEN

Københavns Universitet

Reciprocal mutations of two multifunctional β-amyrin synthases from **Barbarea vulgaris** shift α/β-amyrin ratios

Günther, Jan; Erthmann, Pernille Osterbye; Khakimov, Bekzod; Bak, Søren

Published in:
Plant Physiology

DOI:
10.1093/plphys/kiab545

Publication date:
2022

Document version
Publisher's PDF, also known as Version of record

Document license:
CC BY-NC-ND

Citation for published version (APA):
Günther, J., Erthmann, P. O., Khakimov, B., & Bak, S. (2022). Reciprocal mutations of two multifunctional β-amyrin synthases from *Barbarea vulgaris* shift α/β-amyrin ratios. *Plant Physiology*, *188*(3), 1483-1495. https://doi.org/10.1093/plphys/kiab545

Download date: 02. Jul. 2026

Preprint: Hyperfine Interactions 242, 56 (2021)

Noname manuscript No.
(will be inserted by the editor)

Perturbed Angular Correlation Spectra Due to Rotating Electric Field Gradients

Matthew O. Zacate · Lars Hemmingsen

Received: date / Accepted: date

Abstract The literature on effects of time-dependent hyperfine interactions on perturbed angular correlation (PAC) spectra is dominated by analyses based on models of stochastically fluctuating interactions. The Floquet formalism offers a convenient alternative analysis when interactions have a harmonic time dependence. This is demonstrated in the present work through simulation of PAC spectra due to uniformly rotating electric field gradients (EFGs). Physically, this situation would arise when PAC tracers are embedded in molecules with inertial rotation velocities much larger than molecular collision rates, in which case reorientation of rotation axes would be negligible on the characteristic PAC timescale. The prospect for using PAC to study inertial properties of molecules is explored through simulations with molecules modeled as symmetric, rigid bodies.

Keywords Electric quadrupole interaction · time-dependent Hamiltonian · TDPAC · rotational diffusion

1 Introduction

Among its many uses, perturbed angular correlation (PAC) spectroscopy has been applied to study rotational diffusion of molecules [1–11]. There have been

Funding support for this work was provided in part by the Northern Kentucky University College of Arts and Sciences Professional Development Award.

M. O. Zacate
Department of Physics, Geology, and Engineering Technology, Northern Kentucky University, Highland Heights, KY 41099, USA
Tel.: +001-859-5721365
E-mail: zacatem1@nku.edu

L. Hemmingsen
Department of Chemistry, University of Copenhagen, 2100 København Ø, Denmark

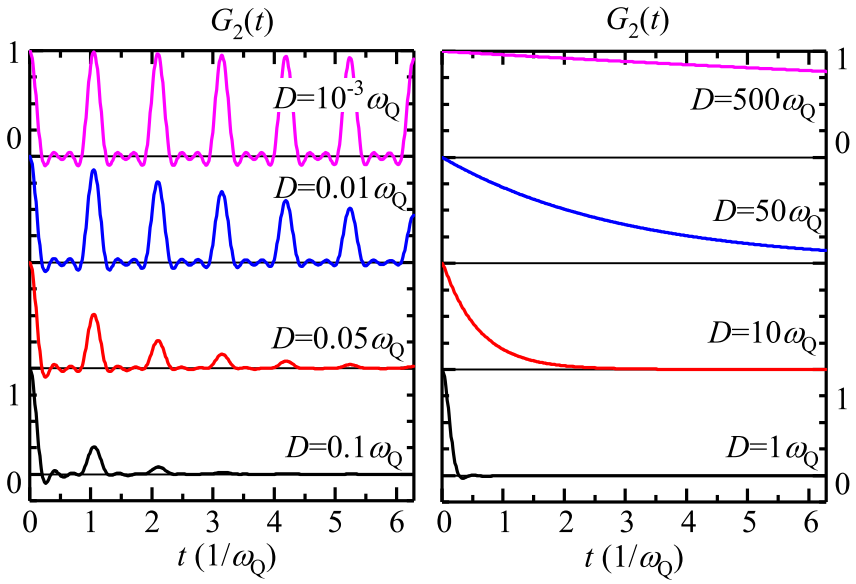

Fig. 1 Simulated PAC spectra for spin-5/2 probes experiencing stochastic reorientation of EFG within the Debye model as calculated using the method of Winkler [14]. Graphs with increasing diffusion coefficient D are arranged counter-clockwise starting from top, left.

two basic approaches for calculating the theoretical PAC perturbation function, $G_2(t)$, to use in fits of spectra obtained when PAC probe atoms are in a molecular environment that produces an electric field gradient (EFG) at the probe site and that EFG reorients due to molecular collisions. One approach is based on the Debye model for rotational diffusion, in which molecular collisions are considered to cause the rotation axis of a molecule to reorient by small angles. Important pioneering work was done by Abragam and Pound in the fast angular rotation regime [12], by Marshall, Werbelow, and Meares in the slow regime [13], and by Winkler [14]. The second approach is based on the strong-collision model, for which collisions lead to Markovian, large-angle reorientations. Early derivations based on this model were developed by Scherer and Blume [15,16] and also by Winkler [14].

Perturbation functions for the Debye diffusion model as calculated using the method of Winkler are shown in Fig. 1. When the rotational diffusion coefficient D is less than or about equal to the interaction frequency that is characteristic of the electric quadrupole interaction, ω_Q, then perturbation functions calculated with these models are characterized by a sum of damped oscillations, $G_2(t) = \sum_n A_n \exp(-\lambda_n t)\cos(\omega_n t)$ where A_n, $\lambda_n \propto D$, and ω_n are the amplitude, relaxation factor, and angular frequency of the nth contribution to the function. For larger diffusion constants, $G_2(t) \propto \exp(-\lambda t)$ where $\lambda \propto 1/D$. Therefore, for very large diffusion coefficients, the perturbation function is in the motionally averaged limit, corresponding to PAC probes experiencing zero EFG, on average, so $G_2(t) = 1$.

Preprint: Hyperfine Interactions 242, 56 (2021)

The stochastic models describe a regime in which molecular collisions occur at rates much larger than rotational velocities of molecules, so time-dependent variations in EFGs experienced by PAC probes are dominated by stochastic reorientation of EFGs. In between collisions, a molecule rotates so that the EFG rotates as well. It is of interest to consider the limit in which collision rates are much smaller than rotational velocity and much smaller than the inverse time-scale of the PAC measurement. In such a case, the measured evolution of the EFG would correspond to rotation only.

The purpose of this work is to derive an expression for $G_2(t)$ that arises due to rotation of an EFG about a fixed axis. For simplicity, only axially symmetric EFGs will be considered. It will be done in the context of considering the source of rotating EFG to be from probes located in molecules that can be described as rigid bodies with the rotational inertia of a symmetric top. First, the physics of symmetric rigid-body rotation will be reviewed. Then, the method for calculating $G_2(t)$ for rotating EFGs will be given. This will be followed by simulations to show how the shape of $G_2(t)$ is influenced by rotational velocity and by orientation of the main, principal EFG axis with respect to the axis of rotation. Then, additional simulations for a distribution of angular velocities will be given in order to explore what one might expect to obtain in experiments when spectra are influenced mainly by molecular rotation and only negligibly by molecular collisions.

2 Review of symmetric rigid-body rotation

The moment-of-inertia tensor $\mathbf{I}$ describes the resistance of a rigid body to change in angular velocity due to an external torque. In the principal axis system, $\mathbf{I}$ of a symmetric rigid body is diagonal with elements $I_1 = I_2 \neq I_3$, where I_3 is the moment of inertia about the unique symmetry axis. For a prolate body, $I_1 > I_3$ and for an oblate body, $I_1 < I_3$.

The physics of rigid-body rotation is well established and results needed for the present work are found readily in textbooks on classical mechanics (refs. [17,18], as examples). For a rigid body with angular momentum $\mathbf{L}$, the orientation of its angular velocity $\boldsymbol{\omega}$ will, in general, differ from the orientation of $\mathbf{L}$, as shown in Fig. 2a. Using the notation of ref. [18], the angle between the unique symmetry axis and $\mathbf{L}$ is θ, and the angle between the symmetry axis and $\boldsymbol{\omega}$ is denoted by α. These angles are related by the moment-of-inertia elements according to

$$\tan\theta = \frac{I_1}{I_3}\tan\alpha. \tag{1}$$

The motion of the body can be described as a combination of two rotations: (1) rotation about the unique symmetry axis with component of angular velocity along this axis, ω_3, and (2) precession of this symmetry axis about $\mathbf{L}$ with angular velocity $\dot{\phi} = L/I_1$, again, using the notation of ref. [18]. In terms of the principal axis system of the moment-of-inertia tensor, the components of angular momentum are given by $\sqrt{L_1^2 + L_2^2} = L\sin\theta$, and

Preprint: Hyperfine Interactions 242, 56 (2021)

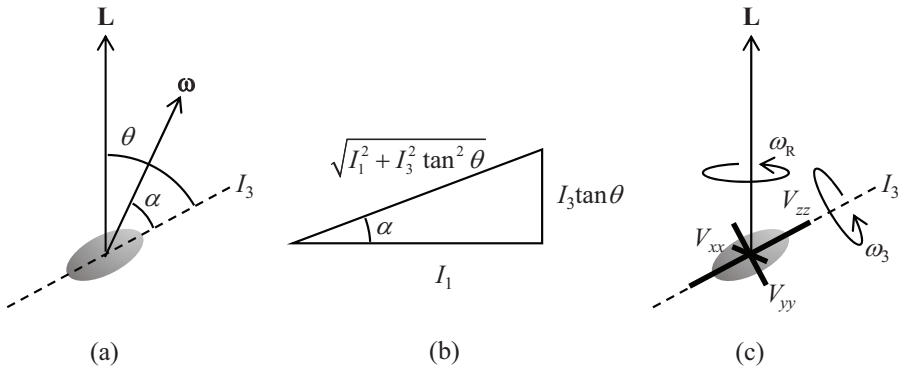

Fig. 2 Geometry of the rotating symmetric rigid body. (a) Angles θ and α relating the angular momentum $\mathbf{L}$, the angular velocity $\boldsymbol{\omega}$, and the principal component of the moment-of-inertia tensor along the unique symmetry axis of the rigid body, I_3. (b) Graphical representation of Eq. 1. (c) Motion of rigid body and EFG with same principal axes as the body's inertia tensor is described by rotation about the symmetry axis and precession about the axis defined by $\mathbf{L}$.

$L_3 = L\cos\theta$. So, $\dot{\phi}$ can be expressed $\dot{\phi} = \omega\sqrt{\sin^2\alpha + I_3^2\cos^2\alpha/I_1^2}$. A graphical representation of Eq. 1 is shown in Fig. 2b, inspection of which reveals $\sin^2\alpha = I_3^2\tan^2\theta/\left(I_1^2 + I_3^2\tan^2\theta\right)$ and $\cos^2\alpha = I_1^2/\left(I_1^2 + I_3^2\tan^2\theta\right)$, so

$$\dot{\phi} = \omega I_3\sqrt{\frac{1+\tan^2\theta}{I_1^2 + I_3^2\tan^2\theta}}. \tag{2}$$

That is, the precession frequency of the rigid body about the angular momentum vector depends on the magnitude of angular velocity, ω, the angle θ, and elements of the moment-of-inertia tensor.

3 Simple rotation of an axially symmetric EFG

For simplicity, this work considers the special case of an axially symmetric EFG with principal axes oriented the same as the moment-of-inertia principal axes and with $V_{zz} \parallel I_3$ as shown in Fig. 2c. In this case, rotation of the body about its symmetry axis with angular velocity ω_3 will not lead to an observable change in EFG, since $V_{xx} = V_{yy}$. Thus, only the precession of the symmetry axis about $\mathbf{L}$ with angular velocity $\omega_R \equiv \dot{\phi}$ leads to observable reorientation of the EFG.

Letting V_0 denote the strength and sign of the EFG, the EFG in its principal axis system is

$$\mathbf{V}' = \begin{pmatrix} -\frac{1}{2}V_0 & 0 & 0 \\ 0 & -\frac{1}{2}V_0 & 0 \\ 0 & 0 & V_0 \end{pmatrix} \tag{3}$$

Preprint: Hyperfine Interactions 242, 56 (2021)

in Cartesian form and has tensor components $V_0^{\prime(2)} = \frac{1}{4}\sqrt{\frac{5}{\pi}}V_0$ and $V_{\pm1}^{\prime(2)} = V_{\pm2}^{\prime(2)} = 0$. Expressed in the coordinate system for which $\mathbf{L}$ is in the z-direction and angle-of-precession is 0 at $t = 0$, the EFG is given in terms of the Wigner D-matrix by $\mathbf{V}(t) = \mathbf{D}(\omega_{\mathrm{R}}t, \theta, \omega_3 t)\,\mathbf{V}'$, which, after evaluation, gives

$$V_0^{(2)}(t) = \frac{1}{8}\sqrt{\frac{5}{\pi}}V_0\left(3\cos^2\theta - 1\right), \tag{4}$$

$$V_{\pm1}^{(2)}(t) = \mp\frac{1}{8}\sqrt{\frac{15}{2\pi}}V_0\sin(2\theta)\exp\left(\mp i\omega_{\mathrm{R}}t\right), \text{ and} \tag{5}$$

$$V_{\pm2}^{(2)}(t) = \frac{1}{8}\sqrt{\frac{15}{2\pi}}V_0\sin^2\theta\exp\left(\mp 2i\omega_{\mathrm{R}}t\right). \tag{6}$$

As expected, Eqs. 4–6 do not depend on ω_3.

The Hamiltonian describing the interaction experienced by a nucleus with quadrupole moment Q and total spin I in an EFG is given by $\langle Im'|H_{\mathrm{Q}}|Im\rangle = \frac{4\pi}{5}\sum_{\mu=-2}^{2}(-1)^{\mu}\left\langle Im\left|q_{\mu}^{(2)}\right|Im'\right\rangle V_{-\mu}^{(2)}$ where

$$\left\langle Im'\left|q_{\mu}^{(2)}\right|Im\right\rangle = (-1)^{I-m}\sqrt{\frac{5}{16\pi}}eQ\begin{pmatrix} I & I & 2 \\ m' & -m & \mu\end{pmatrix}\begin{pmatrix} I & I & 2 \\ I & -I & 0\end{pmatrix}^{-1}. \tag{7}$$

In terms of the quadrupole interaction frequency, $\omega_{\mathrm{Q}} \equiv eQV_{zz}/\left[4I(2I-1)\hbar\right]$,

$$\langle Im'|H_{\mathrm{Q}}|Im\rangle = \hbar\omega_{\mathrm{Q}}c_{mm'I}\sqrt{\frac{3}{2}}\left(3\cos^2\theta - 1\right)^{(-1)}\left[\delta_{m',m\pm2}\sin^2\theta e^{\mp 2i\omega_{\mathrm{R}}t}\right.$$
$$\left.\pm\delta_{m',m\pm1}\sin(2\theta)\,e^{\mp i\omega_{\mathrm{R}}t} + \delta_{m',m}\sqrt{\frac{2}{3}}\left(3\cos^2\theta - 1\right)\right], \tag{8}$$

where

$$c_{mm'I} = (-1)^{I-m}\begin{pmatrix} I & I & 2 \\ m' & -m & m-m'\end{pmatrix}\begin{pmatrix} I & I & 2 \\ I & -I & 0\end{pmatrix}^{-1}. \tag{9}$$

For an ensemble of randomly oriented molecules, the PAC spectrum $G_2(t)$ is given by

$$G_2(t) = \sum_{m_1 m_1' m_2 m_2'}(-1)^{2I+m_1+m_2}\,\delta_{m_1-m_1',m_2-m_2'}\begin{pmatrix} I & I & 2 \\ m_1' & -m_1 & m_1-m_1'\end{pmatrix}\times$$
$$\begin{pmatrix} I & I & 2 \\ m_2' & -m_2 & m-m_2'\end{pmatrix}\langle Im_2|\Lambda(t)|Im_1\rangle\langle Im_2'|\Lambda(t)|Im_1'\rangle^{*} \tag{10}$$

where $\boldsymbol{\Lambda}(t)$ is the evolution, or time-development, operator. The evolution operator is related to the Hamiltonian $\mathbf{H}(t)$ according to

$$\boldsymbol{\Lambda}(t) = \hat{\mathbf{T}}\exp\left[-i\int_0^t \mathbf{H}(t')\,dt'\right], \tag{11}$$

Preprint: Hyperfine Interactions 242, 56 (2021)

where $\hat{\mathbf{T}}$ is the time-ordering operator.

For a time-independent interaction with Hamiltonian $\mathbf{H}$, the evolution operator is simply $\boldsymbol{\Lambda}(t) = \exp(-i\mathbf{H}t)$, and matrix elements appearing in Eq. 10 are given by

$$\langle Im_2| \Lambda(t) |Im_1\rangle = \sum_q \langle Im_2 |q\rangle \exp(-i\lambda_q t) \langle q| Im_1\rangle \tag{12}$$

where λ_q and $|q\rangle$ are the qth eigenvalue and eigenvector of $\mathbf{H}$. This leads to the expression

$$G_2(t) = \sum_n s_n \cos(\omega_n t) \tag{13}$$

where ω_n are distinct differences in eigenvalues λ_q, and s_n arise from sums involving Wigner-3j symbols and projections of eigenvectors on nuclear spin states. For $I = 5/2$, one obtains the familiar $\{s_0, s_1, s_2, s_3\} = \{1/5, 13/35, 2/7, 1/7\}$ and $\{\omega_0, \omega_1, \omega_2, \omega_3\} = \{0, 6\omega_\mathrm{Q}, 12\omega_\mathrm{Q}, 18\omega_\mathrm{Q}\}$ for an axially symmetric electric quadrupole interaction.

A general solution to Eq. 11 for any time dependence is not readily available; however, the Floquet formalism [19,20] provides a useful method of solution for a Hamiltonian that describes an interaction with periodic time dependence. For an interaction with period $2\pi/\omega$, elements in the Hamiltonian will contain Fourier-component factors $\exp(in\omega t)$ where n is an integer. One introduces the Floquet basis $|\alpha, n\rangle \equiv |\alpha\rangle \otimes |n\rangle$, where $|\alpha\rangle$ is the Hamiltonian basis and n is the Fourier component, and the Floquet Hamiltonian $\langle \alpha' n'| H_\mathrm{F} |\alpha n\rangle = \langle \alpha'| H^{(n'-n)} |\alpha\rangle + n\omega\delta_{n'n}\delta_{\alpha'\alpha}$ where $\langle \alpha'| H^{(n)} |\alpha\rangle$ denotes the time-independent factor in the Fourier expansion $\langle \alpha'| H |\alpha\rangle = \langle \alpha'| \sum_n H^{(n)} e^{-in\omega_\mathrm{R} t} |\alpha\rangle$. This allows elements of the evolution operator to be calculated via $\Lambda_{\alpha'\alpha}(t) = \sum_{n,q} \langle \alpha' n|\lambda_q\rangle \exp(-i\lambda_q t) \langle \lambda_q|\alpha 0\rangle \exp(in\omega t)$.

In the present study, the interaction has harmonic time-dependence with angular frequency ω_R, and the Hamiltonian contains factors $\exp(in\omega_\mathrm{R} t)$ with $n = -2, -1, 0, 1, 2$. In this case, the needed Floquet basis is $|Im, n\rangle \equiv |Im\rangle \otimes |n\rangle$ with $n = -4, -3, -2, -1, 0, 1, 2, 3, 4$. And, the Floquet Hamiltonian is given by

$$\begin{aligned}\langle Im', n'| H_\mathrm{F} |Im, n\rangle = \hbar\omega_\mathrm{Q} c_{mm'I} \frac{1}{2} \Bigg[& \left(3\cos^2\theta - 1\right) \delta_{m',m}\delta_{n',n} \\ & \pm \sqrt{\frac{3}{2}} \sin(2\theta)\, \delta_{m',m\pm1}\delta_{n',n\mp1} \\ & + \sqrt{\frac{3}{2}} \sin^2\theta \delta_{m',m\pm2}\delta_{n',n\mp2} \Bigg] + n\hbar\omega_\mathrm{R}\delta_{m',m}\delta_{n',n}.\end{aligned} \tag{14}$$

This gives for the evolution operators appearing in Eq. 10:

$$\langle Im_2| \Lambda(t) |Im_1\rangle = \sum_q \sum_n \langle m_2 n|q\rangle\, e^{-i\lambda_q t} \langle q|m_1 0\rangle\, e^{-in\omega_\mathrm{R} t}, \tag{15}$$

Preprint: Hyperfine Interactions 242, 56 (2021)

where λ_q and $|q\rangle$ are the qth eigenvalue and eigenvector of the Floquet Hamiltonian defined in Eq. 14.

That is, the PAC perturbation function for a rotating axially symmetric EFG will be a function of ω_{Q}, ω_{R}, and θ: $G_2(\omega_{\mathrm{Q}}, \omega_{\mathrm{R}}, \theta, t)$. Its calculation involves constructing the Floquet Hamiltonian defined in Eq. 14, finding the corresponding eigenvalues and eigenvectors to calculate components of the evolution operator in Eq. 15, and substituting those components in Eq. 10. Because the Floquet Hamiltonian is a real, symmetric matrix, the eigenvalues are real and Eqs. 10 and 15 lead to a perturbation function that is a sum of cosines without the exponential damping factors characteristic of perturbation functions calculated using stochastic models.

4 Simulations

The effect of EFG rotation on PAC spectra can be investigated through simulations varying angular velocity ω_{R} and the angle between the EFG main, principal axis and the axis of rotation, θ. Fig. 3 shows PAC spectra for a time range representative of what is typically accessible in measurements for varying precession frequency at $\theta = \pi/2$ and $\theta = \pi/6$. For very low precession frequency ($\omega_{\mathrm{R}} \lesssim 0.01\omega_{\mathrm{Q}}$), the PAC spectrum looks like that obtained for a static electric quadrupole interaction because the rotation speed is much less than the inverse timescale of the PAC measurement. For $0.01\omega_{\mathrm{Q}} \lesssim \omega_{\mathrm{R}} \lesssim 0.3\omega_{\mathrm{Q}}$, PAC spectra have some similarity to spectra obtained using stochastic fluctuation models in the slow fluctuation regime; although, as already stated, spectra using the present rotation model do not have exponential damping factors — the apparent line-broadening is due to a superposition effect arising from multiple oscillations with similar frequencies. This is seen more readily by plotting $G_2(t)$ to larger t as in Fig. 4, which shows a beat pattern characteristic of interference effects. For $\omega_{\mathrm{R}} \gtrsim 1000\omega_{\mathrm{Q}}$, spectra are in the motionally averaged regime where a spectrum is equivalent to the $G_2(t)$ of the static, axially-symmetric EFG that is obtained by averaging the rotating EFG over all orientations.

Dependence on θ of spectra in the motionally averaged regime is shown in Fig. 5a. In each case, $G_2(t)$ is equivalent to the PAC spectrum of a time-independent quadrupole interaction with EFG given by Eqs. 4–6 averaged over one period of rotation. This average is an axially symmetric EFG with main principal component given by $\langle V_{zz}\rangle = \frac{1}{4}V_0\left[1 + 3\cos(2\theta)\right]$. The dependence of $\langle V_{zz}\rangle$ on θ is shown in Fig. 5b. In the one extreme, $\theta = 0$, the motionally-averaged interaction is identical to the underlying EFG, because there is no reorientation of the V_{zz} component; moreover, $G_2(t)$ will have no dependence on ω_{R} in this limit. On the other extreme, $\theta = \pi/2$, $\langle V_{zz}\rangle$ is the same as V_{yy}, because this component of the EFG remains parallel to $\mathbf{L}$ throughout the period of rotation. The cross-over between positive and negative values of $\langle V_{zz}\rangle$ occurs at $\theta = \cos^{-1}\left(1/\sqrt{3}\right)$, which is the angle between the body

Preprint: Hyperfine Interactions 242, 56 (2021)

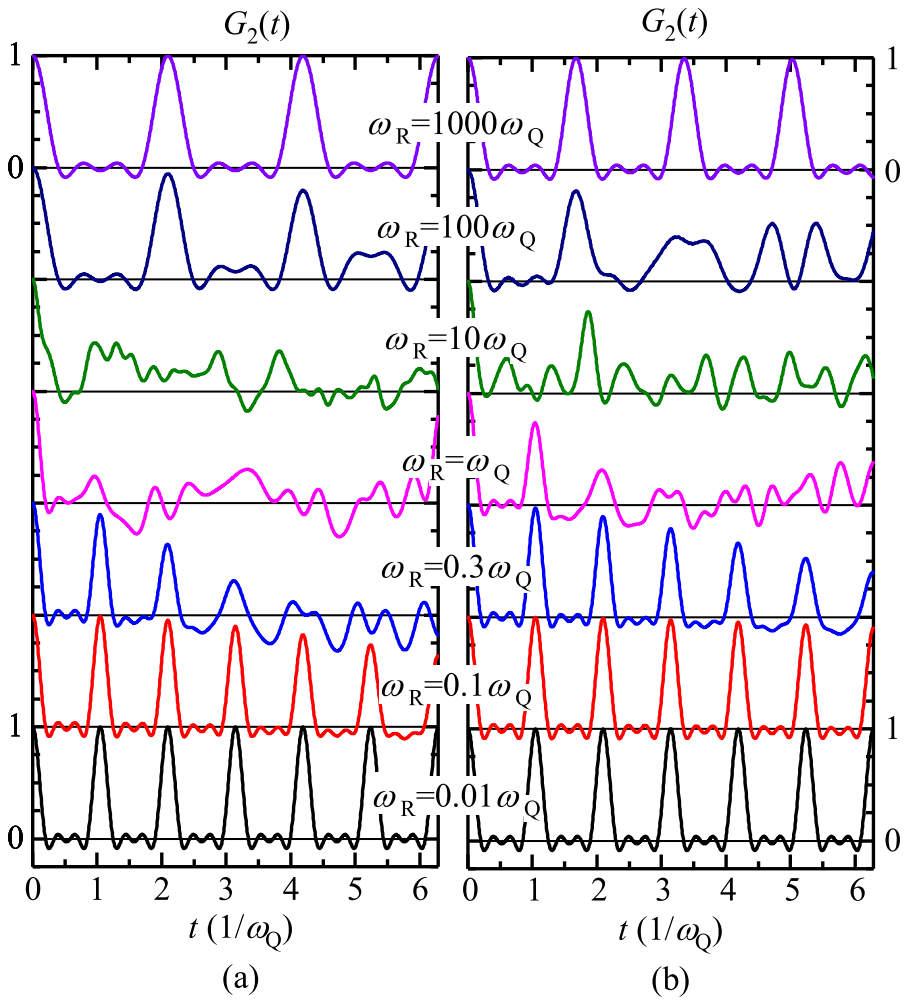

Fig. 3 Simulated PAC spectra for a spin-5/2 probe experiencing a rotating EFG with indicated rotation frequencies ω_R at (a) $\theta = \pi/2$ and (b) $\theta = \pi/6$.

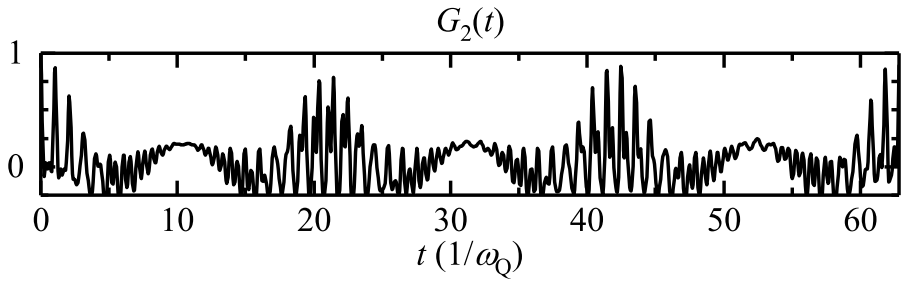

Fig. 4 Simulated PAC spectrum for a spin-5/2 probe with $\omega_R = 0.3\omega_Q$ and $\theta = \pi/2$, showing behavior over a long time period.

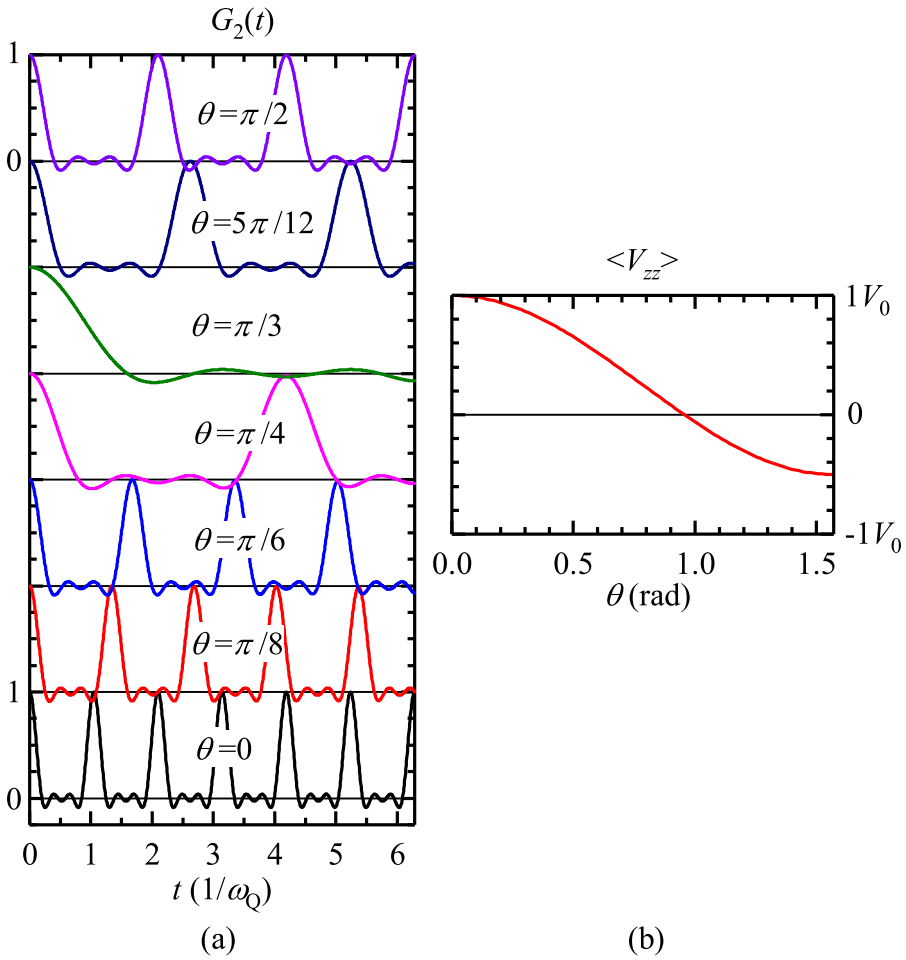

Fig. 5 Simulated PAC spectrum for a spin-5/2 probe with $\omega_R = 1000\omega_Q$, showing (a) behavior in the motionally averaged limit, at indicated values of θ, and (b) value of main principal component of the time-averaged EFG, $\langle V_{zz}\rangle$, as a function of θ.

diagonal and edge of a cube. At this angle, the motionally averaged spectrum is unperturbed; *i.e.*, $G_2(t) = 1$.

5 Simulation of spectra for symmetric molecules rotating with a distribution of angular velocities

Simulations in the previous section show effects of rotating EFGs on $G_2(t)$, independent of the physical origin of the rotating EFG. One possible physical realization of the rotating EFG would be when PAC probe nuclei are located in an ensemble of molecules. If it is possible to achieve experimental conditions such that the average time between molecular collisions is much larger than

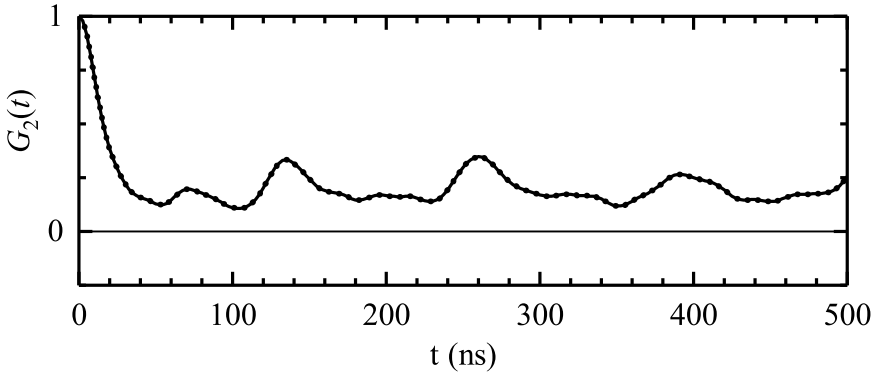

Fig. 6 Simulated PAC spectrum for a spin-5/2 probe experiencing distributions of ω_{R} and θ expected for $I_1 = 1.9 \times 10^{-44}$ kg $\cdot$ m^2, $I_3 = 3.8 \times 10^{-44}$ kg $\cdot$ m^2, and $\omega_{\mathrm{Q}} = 16.8$ Mrad/s at $T = 300$ K: full simulation (solid curve) and average of static $G_2(t)$ (dots).

the PAC time scale, perhaps in a gas at low pressure, then one would expect the PAC spectrum to arise from probes in molecules rotating with angular velocity components given by the Maxwell Boltzmann distribution [21]

$$P\left(\omega_1, \omega_2, \omega_3\right) = \sqrt{\frac{I_1^2 I_2}{8\left(\pi k_{\mathrm{B}} T\right)^3}} \exp\left[-\left(I_1\omega_1^2 + I_1\omega_2^2 + I_3\omega_3^2\right)/2k_{\mathrm{B}}T\right]. \quad (16)$$

In this case, the measured PAC perturbation function would be given by

$$\begin{aligned}\left\langle G_2\left(\omega_{\mathrm{Q}}, t\right)\right\rangle = & \int_{-\infty}^{\infty} d\omega_1 d\omega_2 d\omega_3 P\left(\omega_1, \omega_2, \omega_3\right) \times \\ & G_2\left(\omega_{\mathrm{Q}}, \omega_{\mathrm{R}}\left(\omega_1, \omega_2, \omega_3\right), \theta\left(\omega_1, \omega_2, \omega_3\right), t\right). \end{aligned} \quad (17)$$

Molecular moments of inertia are roughly of the order 10^{-44} kg$\cdot$m^2. Choosing values $I_1 = 1.9 \times 10^{-44}$ kg$\cdot$m^2 and $I_3 = 3.8 \times 10^{-44}$ kg$\cdot$m^2 to represent an oblate molecule, $\omega_{\mathrm{Q}} = 16.8$ Mrad/s to represent a moderately strong EFG, and $T = 300$ K, $\left\langle G_2\left(\omega_{\mathrm{Q}}, t\right)\right\rangle$ was calculated using Gauss-Hermite quadrature with 128 points in each dimension and is shown in Fig. 6. The root mean square angular velocity in this example is about 1×10^5 Mrad/s, which is much larger than ω_{Q}. This means that it should be possible to calculate $\left\langle G_2\left(\omega_{\mathrm{Q}}, t\right)\right\rangle$ using a distribution of static perturbation functions with motionally-averaged quadrupole interaction frequencies:

$$\begin{aligned}\left\langle G_2\left(\omega_{\mathrm{Q}}, t\right)\right\rangle = & \int_{-\infty}^{\infty} d\omega_1 d\omega_2 d\omega_3 P\left(\omega_1, \omega_2, \omega_3\right) \times \\ & G_2\left(\frac{1}{4}\omega_{\mathrm{Q}}\left(1 + 3\cos\left[2\theta\left(\omega_1, \omega_2, \omega_3\right)\right]\right), t\right). \end{aligned} \quad (18)$$

The $\left\langle G_2\left(\omega_{\mathrm{Q}}, t\right)\right\rangle$ calculated using Eq. 18 is shown in Fig. 6 and exactly reproduces the spectrum calculated using Eq. 17, as expected.

Preprint: Hyperfine Interactions 242, 56 (2021)

The time dependence in Fig. 6 differs from the exponentially damped spectra characteristic of stochastic models such as are shown in Fig. 1. This means that it should be possible to distinguish between signals obtained from probes in molecules experiencing negligible collisions on the time-scale of the measurement (rotation-only) and in molecules experiencing significant collisions (stochastic reorientation). If it is possible to achieve the experimental condition needed for negligible collision, then it should be possible to use this method to characterize the inertial properties of molecules in which probes are embedded.

The predicted dependence of spectra on ratio I_3/I_1 is shown in Fig. 7. For $0.5 \lesssim I_3/I_1 \leq 2$, the perturbation function is characterized by a broad linewidth, originating from a wide distribution of θ. In this range, the shape of $G_2(t)$ shows a slight dependence on the value I_3/I_1, most visible in the first 150 ns for the selected simulation parameters. For $I_3/I_1 \leq 0.5$, line-broadening decreases with decreasing I_3/I_1, and, correspondingly, the distribution of θ narrows. In the limit of a perfectly prolate molecule ($I_3/I_1 = 0$), only the value $\theta = \pi/2$ is allowed, and the PAC spectrum will be the same as that produced by the motionally averaged EFG with half the interaction frequency of the rotating EFG (see discussion of Fig. 5b in section 4). As seen in Fig. 7, even with a small deviation from perfectly prolate ($I_3/I_1 = 10^{-4}$), the spectrum exhibits the motionally averaged signal within the displayed time range.

6 Discussion

Design of experiments to achieve rotational EFG frequencies in the roughly 10^5–10^9 rad/s range needed to test the predicted rotation-frequency dependence of $G_2(t)$ shown in Fig. 3 is not trivial. A mechanical solution may provide access to the low end of the range. Devices used in magic-angle spinning (MAS) nuclear magnetic resonance measurements are capable of reaching 10^5 Hz [22,23]. Thus, performing a PAC measurement with ^{111}In in indium metal using an MAS device could achieve up to about $0.2\omega_Q$, which, with good counting statistics, should produce an observable effect if the single-crystal sample is mounted so that $\theta = \pi/2$. A chemical solution may provide the means of achieving rotational frequencies throughout the target range; for example, investigation of rotational dynamics of caged supramolecular dynamers using experiment and molecular dynamics simulation [24,25] showed rotation frequencies between 10^{-1} and 10^9 Hz are expected over a temperature range of 66–400 K.

Investigation of the motionally averaged rotation regime may be more readily achievable through PAC experiments with PAC tracers embedded in molecular gasses. A recent PAC study of Hg and Cd halides showed the effect of molecular collisions on signal was relatively minor compared to molecular rotation and vibration effects [11]. If it is necessary to reduce the effects of collisions in order to investigate predicted I_3/I_1 dependence shown in Fig. 7,

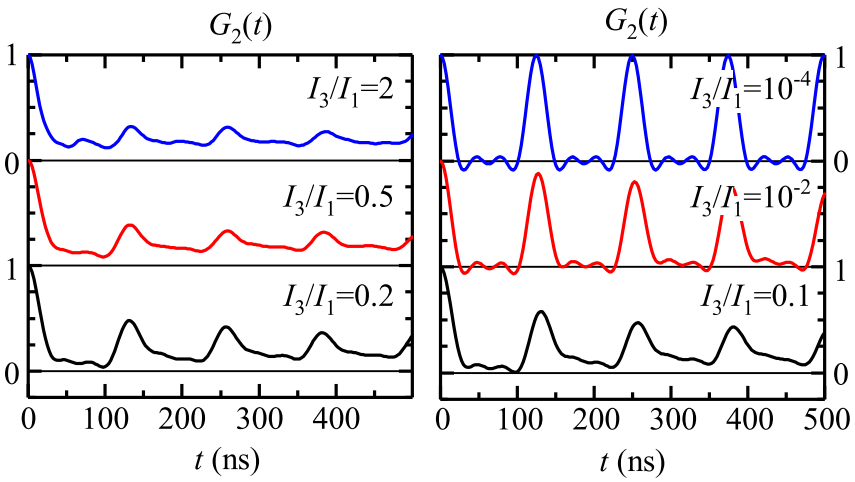

Fig. 7 Simulated PAC spectra expected for a spin-5/2 probe experiencing distributions of ω_R and θ at varying ratios I_3/I_1 with $\max(I_1, I_3) = 1 \times 10^{-44}$ kg $\cdot$ m^2, $\omega_Q = 16.8$ Mrad/s, and $T = 300$ K. Graphs with decreasing I_3/I_1 are arranged counter-clockwise starting from top, left.

then use of the supersonic jet technique might result in molecular gasses with collision time much larger than the inverse rotational frequency [26].

7 Summary

This work showed how to use the Floquet formalism to calculate the PAC perturbation function for tracers that experience rotating EFGs. Only the case of axially symmetric EFGs with principal axis system the same as the principal axis system of the molecular inertia tensor was considered; however, the method is readily adaptable to non-axially symmetric EFGs with any orientation. In that case, the perturbation function is expected to depend on ω_3, the rate of rotation about the unique moment-of-inertia axis, unlike the calculations of this work.

Simulations that included physically appropriate Maxwell-Boltzmann distributions of angular velocities showed that the shape of the perturbation function depends on the ratio of moment-of-inertia components. This indicates that PAC measurements could be used to probe inertial properties of molecules, provided that it is possible to create the physical conditions necessary for the time between molecular collisions to be much larger than the characteristic PAC timescale.

Acknowledgements This work was supported in part by the Sabbatical Leave Program and the College of Arts and Sciences Professional Development Award at Northern Kentucky University.

References

1. Andrade, P.D.R., Vasquez, A., Rogers, J.D., Fraga, E.R.: Nuclear relaxation in $(NH_4)_3HfF_7$ studied by gamma-gamma angular correlation. Physical Review B **1**(7), 2912 (1953)
2. Shirley, D.A.: Estimates of correlation times of dissolved complexes from "rotational tracer" experiments. Journal of Chemical Physics **53**, 465 (1970)
3. Wagner, H.F., Popp, M., Forker, M.: Determination of nuclear multipole relaxation times by measurements of statistically perturbed angular correlations. Z. Physik **248**, 195 (1971)
4. Gerdau, E., Birke, J., Winkler, H., Braunsfurth, J.: Time-dependent electric quadrupole interactions in $(NH_4)_3HfF_7$. Z. Physik **263**, 5 (1973)
5. Baudry, A., Boyer, P., Vulliet, P.: PAC study of molecular reorientations in liquids. Hyperfine Interactions **2**, 279 (1976)
6. Baudry, A., Boyer, P., Fabris, J.D., Vulliet, P.: PAC study of molecular rotational motions in dilute solutions. Hyperfine Interactions **10**, 1057 (1981)
7. Danielsen, E., Bauer, R.: Analysis of perturbed angular correlation spectra of metal ions bound to proteins with rotational correlation times in the intermediate region. Hyperfine Interactions **62**, 311 (1990)
8. Danielsen, E., Bauer, R., Schneider, D.: Rotational correlation times of peptides determined by perturbed angular correlations of γ-rays. European Biophysics Journal **20**, 193 (1991)
9. Hemmingsen, L., Sas, K.N., Danielsen, E.: Biological applications of pertrubed angular correlations of γ-ray spectroscopy. Chemical Reviews **104**, 4027 (2004)
10. Chakraborty, S., Pallada, S., Pedersen, J.T., Jansco, A., Correia, J.G.: Nanosecond dynamics at protein metal sites: An application of perturbed angular correlation (PAC) of γ-rays spectroscopy. Accounts of Chemical Research **50**, 2225 (2017)
11. Haas, H., Röder, J., Correia, J.G., Schell, J., Fenta, A.S., Vianden, R., Larsen, E.M.H., Aggelund, P.A., Fromseger, R., Hemmingsen, L.B.S., Sauer, S.P.A., Lupascu, D.C., Amaral, V.S.: Free molecule studies by perturbed $\gamma - \gamma$ angular correlations: A new path to accurate nuclear quadrupole moments. Physical Review Letters **126**, 103001 (2021)
12. Abragam, A., Pound, R.V.: Influence of electric and magnetic fields on angular correlations. Physical Review **92**, 943 (1953)
13. Marshall, A.G., Werbelow, L.G., Meares, C.F.: Effect of molecular shape and flexibility on gamma-ray directional correlations. The Journal of Chemical Physics **57**(1), 364 (1972)
14. Winkler, H.: $\gamma\gamma$ angular correlations perturbed by randomly reorienting hyperfine fields. Z. Physik A **276**, 225 (1976)
15. Scherer, C.: Gamma-gamma angular correlations: A model for statistical perturbation with any correlation time. Nuclear Physics **A157**, 81 (1970)
16. Blume, M.: Perturbed angular correlations: Perturbation factor for arbitrary correlation time. Nuclear Physics **A167**, 81 (1971)
17. Fetter, A.L., Walecka, J.D.: *Theoretical Mechanics of Particles and Continua* (McGraw-Hill Publishing Company, 1980)
18. Thornton, S.T., Marion, J.B.: *Classical Dynamics of Particles and Systems*, 5th edn. (Brooks/Cole—Thompson Learning, 2004)
19. Shirley, J.H.: Solution of the Schrödinger equation with a hamiltonian periodic in time. Physical Review **138**(4B), 979 (1965)
20. Chu, S.I., Telnov, D.A.: Beyond the floquet theorem: generalized floquet formalisms and quasienergy methods for atomic and molecular multiphoton processes in intense laser fields. Physics Reports **390**, 1 (2004)
21. Hubbard, P.S.: Angular velocity of a nonspherical body undergoing rotational brownian motion. Physical Review A **15**(1), 329 (1977)
22. Samoson, A., Tuherm, T., Reinhold, A., Heinmaa, I., in *New Techniques in Solid-State NMR*, *Topics in Current Chemistry*, vol. 294, ed. by J. Klinowski (Springer, 2005), pp. 15–31

23. Nishiyama, Y., in *Experimental Approaches of NMR Spectroscopy*, ed. by T.N.M.R.S. of Japan (Springer, 2018), pp. 171–195
24. Kühne, D., Klappenberger, F., Krenner, W., Klyatskaya, S., Ruben, M., Barth, J.V.: Rotational and constitutional dynamics of caged supramolecules. Proceedings of the National Academy of Sciences **107**(50), 21332 (2010)
25. Palma, C.A., Björk, J., Rao, F., Kühne, D., Klappenberger, F., Barth, J.V.: Topological dynamis in supramolecular rotors. Nano Letters **14**, 4461 (2014)
26. Ito, M., Ebata, T., Mikami, N.: Laser spectroscopy of large polyatomic molecules in supersonic jets. Annual Review of Physical Chemistry **39**, 123 (1988)